energies

MDPI

Article

Influence of DC Electric Field on the Propane-Air Diffusion Flames and NO_x Formation

Sang-Min Kim [1,*], Kyeong-Soo Han [2] and Seung-Wook Baek [3]

[1] Accident Monitoring and Mitigation Research Team, Korea Atomic Energy Research Institute, Daejeon 34057, Korea
[2] Department of Aerospace Engineering, University of Michigan, Ann Arbor, MI 48109, USA; kshan@umich.edu
[3] Department of Aerospace Engineering, Korea Advanced Institute of Science and Technology, Daejeon 34141, Korea; swbaek@kaist.ac.kr
* Correspondence: ksm0226@kaeri.re.kr; Tel.: +82-10-6566-1355

Abstract: The aim of this research is to investigate the effects of a direct current (DC) electric field on the combustion behavior of a co-flow propane diffusion flame. The flame length and NO_x emission were observed and measured. The electric field enhances the combustion process of propane diffusion flame by causing the movement of ions and molecules in the flame, resulting in a change in the shape of the flame. The flame heights decrease with an increase in the applied voltage and polarity, a more dominant effect to be observed with a positive DC electric field. However, for the applied negative polarity, the inner-cone of the propane diffusion flame is shifted by the electric field. Drastic reduction in the NO_x emission is observed with an increase in the applied DC voltage and polarity. In the existing system, the reduction percentage of NOx is within the range of 55 to 78%.

Keywords: diffusion flame; propane; voltage; polarity; electric field; NO_x

check for updates

Citation: Kim, S.-M.; Han, K.-S.; Baek, S.-W. Influence of DC Electric Field on the Propane-Air Diffusion Flames and NO_x Formation. *Energies* **2021**, *14*, 5745. https://doi.org/10.3390/en14185745

Academic Editor: Yonmo Sung

Received: 19 August 2021
Accepted: 8 September 2021
Published: 13 September 2021

Publisher's Note: MDPI stays neutral with regard to jurisdictional claims in published maps and institutional affiliations.

1. Introduction

Electric control of combustion may optimize energy efficiency, emission control, and fuel flexibility. The hydrocarbon combustion flame contains a large number of ions and electrons with a number density of 10^9–$10^{12}/cm^3$ due to chemi-ionization in the reaction zone, which, in turn, affects the combustion behavior. Hence, by the application of the electric field, the flame combustion dynamics including combustion stability, combustion efficiency, and exhaust emissions can be modified. The dominant ions in the flame of hydrocarbon fuels are cations such as CHO^+, $C_3H_3{}^+$, and $C_2H_3O^+$. The concentration of electrons or negative ions such as $O_2{}^-$ and OH^- depends on the mixing ratio with air. [1–4].

During the combustion process, nitrogen (N_2) in a high-temperature zone of a flame flow tends to react with oxygen (O_2) forming NO and NO_2. In general, NO_x can be formed in three ways. Firstly, thermal NO_x is formed during the combustion of gases and fuels (oils) at a high temperature in a flame, when dissociated oxygen reacts with atmospheric nitrogen [5,6]. Secondly, NO_x is generated by the reaction between hydrocarbon radicals and nitrogen contained in the fuel. Lastly, prompt NO_x is produced rapidly when fuel is exposed to a higher temperature than 1000 °C in a high concentration state of fuel before it is completely mixed with air. Clean combustion control techniques include methods of low excess air firing, combustion of low nitrogen fuel oil, different modifications of burner construction, etc. The simplest method of reducing NO_x is to use a water injection into the combustion zone of a flame and H_2O_2 injection into a hot flue gas stream [7].

The factor that greatly influences NO_x production is the length of the flame. In the case of burning the same amount of fuel, the instability of the flame increases as the length of the flame increases, which affects the soot and NO_x generation [8–11]. The longer the flame length is, the longer the survival time of the flame will be. The longer the flame survival time is, the longer the reaction time with nitrogen in the air will be; therefore, the probability of generating thermal NO_x increases.

This concept of combustion through using the electric fields is a promising technique in achieving clean combustion through a reduction of emissions such as NO_x and other pollutants from combustion. Electric field effects depend on the electric field configuration and polarity, while it can be regulated by varying high voltage DC/AC power supply. Through electrically controlled combustion, a variation of flame temperature can be achieved, affecting the mass fraction distribution in the flame by improving the fuel mixing with oxygen and can cause the change in flame dynamics [12–16]. In addition, the ionic wind effect present in the combustion process by application of an electric field improves flame efficiency. Therefore, the electric field effect shows a very promising effect to improve the combustion stability and efficiency of the flame [17,18]. Equation (1) gives the general relation between the diffusion coefficient and the length of the flame [8,9,19], where H is the length of the flame, T_0 is the ambient temperature, T_f is the flame temperature, s is the air-fuel ratio, Q is the volumetric flow rate of fuel, and D is the diffusion coefficient; that is, as the diffusion coefficient increases, the length of the flame becomes shorter.

$$H = \left(\frac{\left(T_0 / T_f \right)^{0.67}}{4\pi D ln\left(1 + \frac{1}{s}\right)} \right) Q \tag{1}$$

The change in the diffusion coefficient of gaseous ions due to the electric field can be inferred from the Einstein relation (Equation (2)).

$$eD/\mu = k_B T \tag{2}$$

$$\frac{eD_L}{\mu} = k_B T_L \left(1 + \frac{dln\mu}{dln\left(\frac{E}{N}\right)} \right) \tag{3}$$

$$eD_T/\mu = k_B T_T \tag{4}$$

In the equations above, e is the charge number of ion, k_B is the Boltzmann constant, T is the absolute temperature, N is the number density, μ is the mobility of the ion (m^2/sV), and E is the electric field strength (V/m). Equation (3) is the diffusion coefficient in the direction parallel to the electric field, and Equation (4) is the diffusion coefficient in the direction perpendicular to the electric field. The energy increases, as shown in Equations (5) and (6) below, due to collisions among ions and molecules and an increase in flow velocity due to the electric field [20,21].

$$k_B T_L = k_B T_0 + \left(\frac{5m - (2m - M)A^*}{5m + 3MA^*} \right) M (v_d)^2 \tag{5}$$

$$k_B T_T = k_B T_0 + \left(\frac{(m + M)A^*}{5m + 3MA^*} \right) M (v_d)^2 \tag{6}$$

where m is the mass of the ion, M is the mass of the molecule, and A^* is the collision rate between the ion and the molecule; that is, the diffusion coefficient increases in proportion to the kinetic energy of moving molecules due to collision with ions.

A study on the change in diffusion flame characteristics in an electric field has been conducted until recently; Kim [22] and Chien [23] studied both the shape of the flame and the effect on heat transfer. Additionally, Farraj [24] and Pu [25] successfully simulated the shape change of the flame by applying the body force term of the ionic wind to the momentum equation.

The interaction between the electric field and the flame also worked in the premixed flame. Li [26] and Fang [27] investigated the effect of electric field on methane-air mixture premix flame experimentally. The deformation process of the spherically expanding premixed flame was observed, and the application of an electric field commonly promotes flame propagation and increases the heat release rate.

This article focused on studying the behavior of propane-air diffusion flame when subjected to DC electric field over the voltage range of −5 to +5 kV. In particular, efforts were made to investigate the flame dynamics when different applied voltage and polarity were applied at different fuel-air flow rates. Based on previous research, this study aimed to understand and investigate the application of DC voltage and polarity through a radial electrode, generating an electric field in the same or opposite direction of the flame flow, on propane diffusion flame dynamics in terms of flame shape, lowest hot region of flame, flame reaction zone width, flame hot temperature region, and finally, the NO_x generation.

The difference from the previous studies about the interaction between e-field and flame is that in this study, a ring-type electrode was used so that it made e-field concentrate on the diffusion flame's reaction zone. Additionally, based on this difference, correlations were derived between the changes in flame length by e-field and $EINO_x$.

2. Experimental Setup

In this paper, Figure 1 illustrates a schematic diagram of the experimental setup for propane diffusion flame combustion tests by application of electrostatic voltage. The closed chamber used in the experiment has dimensions of 0.5 m × 0.5 m and 0.75 m in height. A grounded burner with a diameter of 42 mm for establishing diffusion flame was made of stainless steel. The outlet of the burner was divided into three parts in the direction of the concentric circle. Pure propane was supplied at the central outlet with a diameter of 6 mm. A mass flow controller (Line Tech M3100V) supplied the fuel at a rate of 0.25, 0.5, and 1 L/min. At the second outlet from the center, the dry air was supplied by the mass flow controller at 12 L/min. At the burner exit, the Reynolds number of this flow is about 900, which is the laminar flow region. Fuel-lean (equivalence ratio: 0.5), stoichiometry (equivalence ratio: 1), and fuel-rich (equivalence ratio: 2) flame were formed depending on the fuel supply. All cases of the experiment can be seen in Table 1.

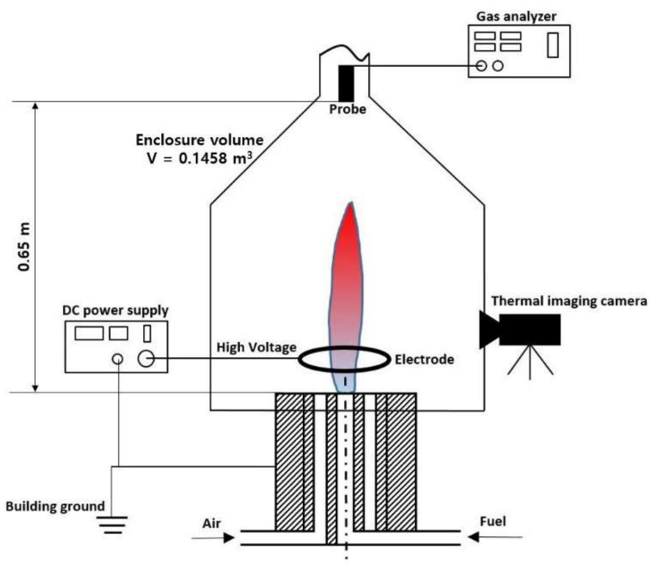

Figure 1. Experimental setup.

Table 1. Experimental conditions.

Voltage Polarity	Case	Fuel Flow Rate (L/min)	Air Flow Rate (L/min)	Equivalence Ratio
Positive (+)	Stoichiometry	0.5	12	1
	Rich	1		2
	Lean	0.25		0.5
Negative (−)	Stoichiometry	0.5	12	1
	Rich	1		2
	Lean	0.25		0.5

High-resolution IR camera set to capture the temperature distribution data within the propane diffusion flame. Changes in the temperature profile and flame dynamics were observed by thermal imaging (infrared) camera (Fluke Ti400). The IR camera had an infrared spectral band from 7.5 µm to 14 µm. The range of wavelength emitted varied as an object's temperature changed, and the sensor detected its wavelength emitted. Then, based on the strength of the wavelength, the appropriate colors were displayed on a screen. The IR emissivity of the flame surface was set to 1. The purpose of this research is to focus on the flame length change more than obtaining precisely measured flame temperature. Therefore, slight errors did not affect the results of this study.

A high voltage power supply (GLASSMAN HIGH VOLTAGE INC. EK series) with a ring-type electrode (Figure 2) of 26.5 mm in inner diameter and 3.25 mm in thickness was adjusted at 25 mm height from burner exit to generate electric field and polarity of −5 to +5 kV. The high voltage power source was able to supply direct-current voltage from 0 to 5 kV.

(**a**)

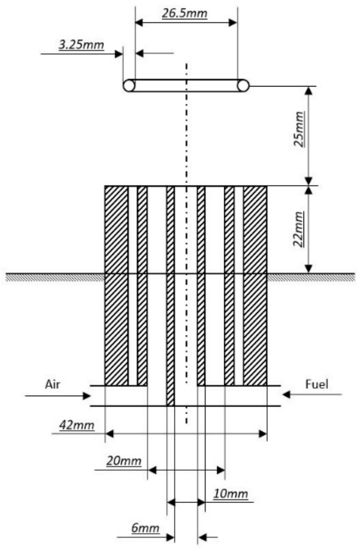

(**b**)

Figure 2. (**a**) Burner and electrode; (**b**) size and location in detail.

The NO_x was measured by installing a gas analyzer probe (EUROTRON Greenline) on the exhaust portion of the combustion chamber (Figure 1). The probe is located at a height of 65 cm from the burner surface. It is possible that the exhaust gas is diluted by the fresh air in the container. Therefore, we used values that were measured after ignition, and we waited until the inside of the enclosure became stable and uniform case by case.

The intensity and direction of the electric field generated by the electrode were demonstrated by using the Ansys Maxwell 2D program (Figure 3).

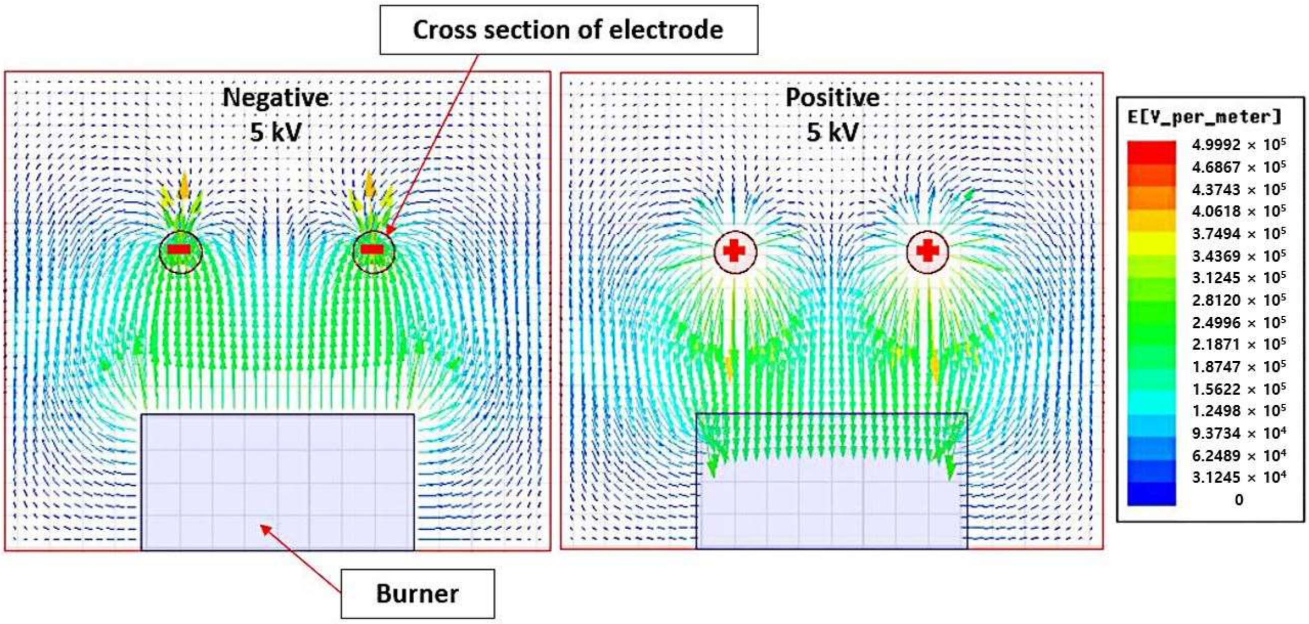

Figure 3. Demonstration of force and direction of electric field generated by radially positioned electrode.

3. Results

The main focus of this research was to understand the effect of applied voltage and polarity on the flame dynamics of the propane diffusion flame. To understand this phenomenon, the following experimentation was performed, as discussed in subsequent sections.

3.1. Flame Shape and Length

Efforts were made to understand the electric field within the flame due to the application of the applied voltage and polarity (negative or positive) (Figure 3). Figure 3 shows that there is a different direction of the electric field within the flame for the applied positive and negative voltage.

For the negative polarity case, the direction of the electric field is upward from the burner exit, while for the positive polarity, the direction of the electric field is toward the burner exit. Among charged ions inside the flame, the positive ions move in the same direction as the electric field. The cations generated from the pyrolysis of fuel are dense in the blue region, which is why this area is most affected by electric fields. With an increase in the applied negative polarity, the positive ions move away from the burner exit. It is also observed that the blue region (reaction zone) of the applied negative polarity is stretched with an increase in voltage through the electrode, as seen in Figure 4, whereas in the blue region of the positive polarity, the blue region becomes shorter but thicker.

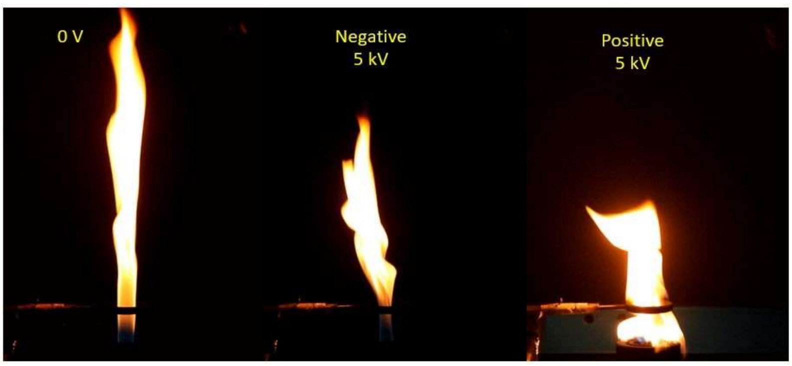

Figure 4. The change in flame shape by electric field.

Figure 5 is an image taken with an infrared thermal imaging camera of the shape of the flame that changes when a positive voltage is applied to the electrode. When no electric field is applied, it can be seen that the flame length is shorter in the fuel-lean case (c) than in cases (a) and (b). The length of the coaxial diffusion flame is proportional to the fuel flow rate and inversely proportional to the diffusion coefficient and air-fuel ratio, as was discussed in Equation (1) in the Introduction Section.

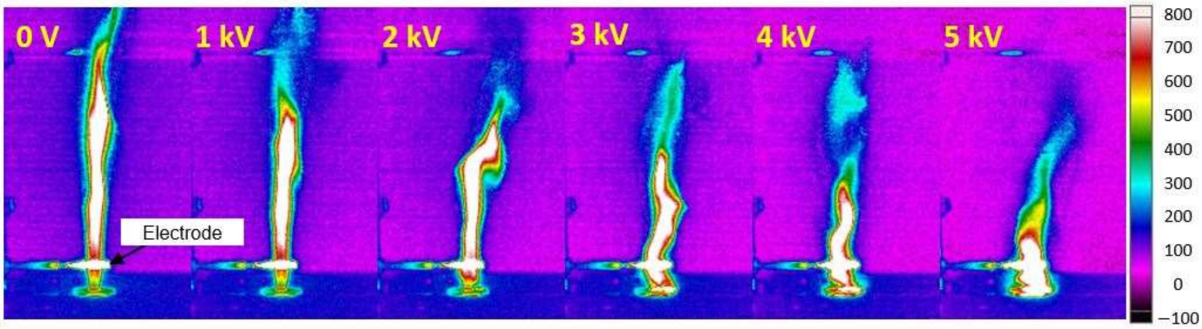

(**a**) Stoichiometry case (air 12 L/min, fuel 0.5 L/min).

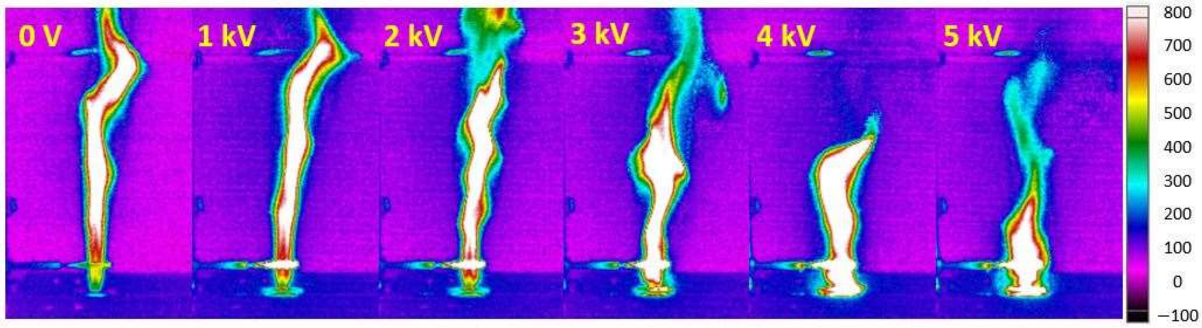

(**b**) Fuel-rich case (air 12 L/min, fuel 1 L/min).

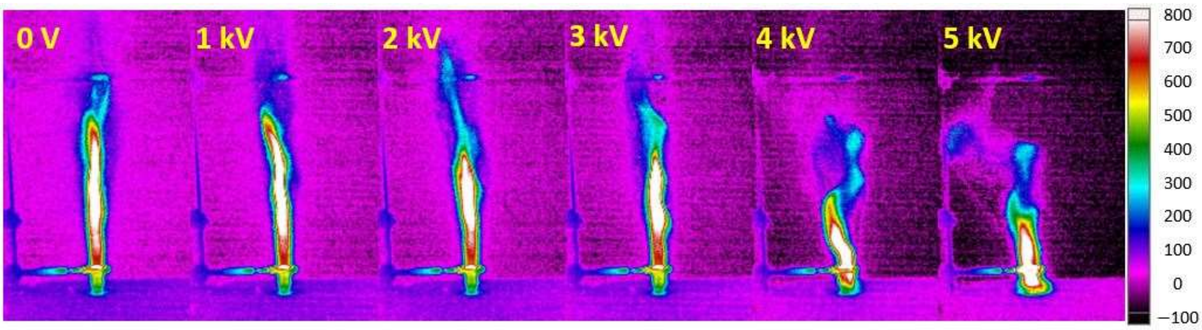

(**c**) Fuel-lean case (air 12 L/min, fuel 0.25 L/min).

Figure 5. Infrared image for positive polarity (°C): (**a**) stoichiometry case; (**b**) fuel-rich case; (**c**) fuel-lean case.

In the reaction zone between the electrode and the burner surface, an electric field acting in the opposite direction to the direction of the flame is formed, and the turbulence increases as the voltage increases due to the conflict between the body force of the ionic wind that presses the flame downward and the fuel ejected upward.

Figure 6 shows the shape of the flame that changes when a negative voltage is applied to the electrode. In all cases (a), (b), and (c), the flame length became shorter as the voltage applied to the electrode increased. In all cases under the same voltage, as the amount of fuel supplied increased, the length of the flame was longer. As in the case where the electrode was positively charged, the diffusion coefficient of the flame increased due to the electric field acting in the direction parallel to the direction of the flame in the reaction zone of the flame, and thus, the length of the flame was reduced (Equations (1)–(6)). However, it showed a stable appearance without increasing turbulence, compared to when a positive electric field was applied in all areas and the reaction zone of the flame.

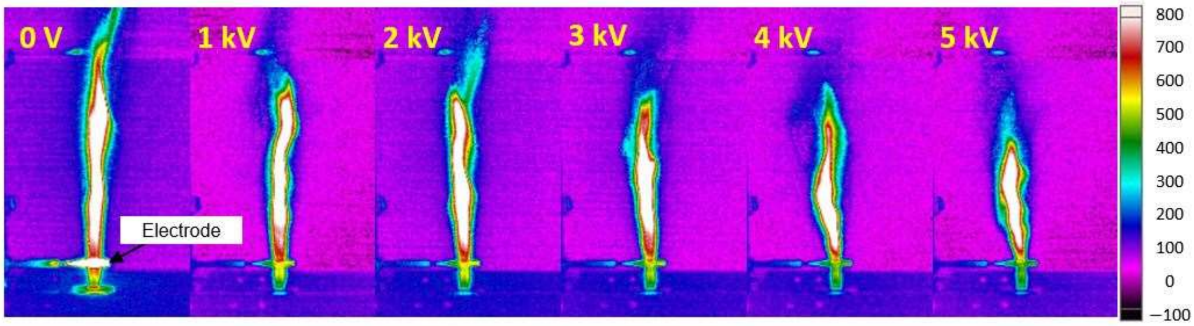

(**a**) Stoichiometry case (air 12 L/min, fuel 0.5 L/min).

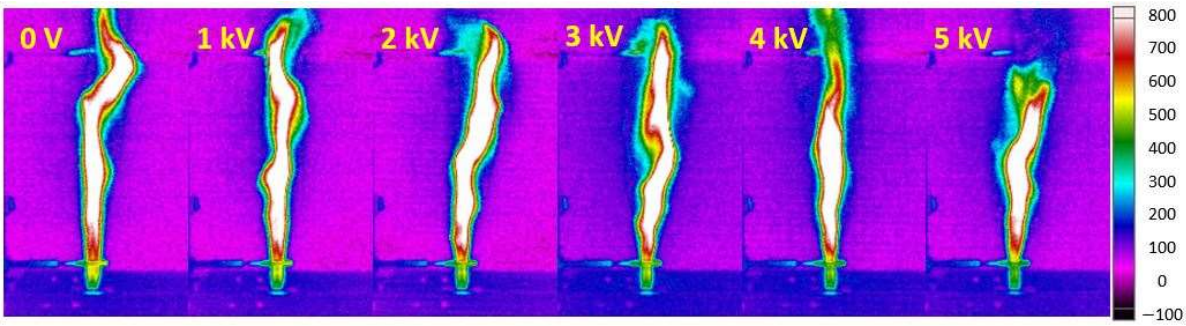

(**b**) Fuel-rich case (air 12 L/min, fuel 1 L/min).

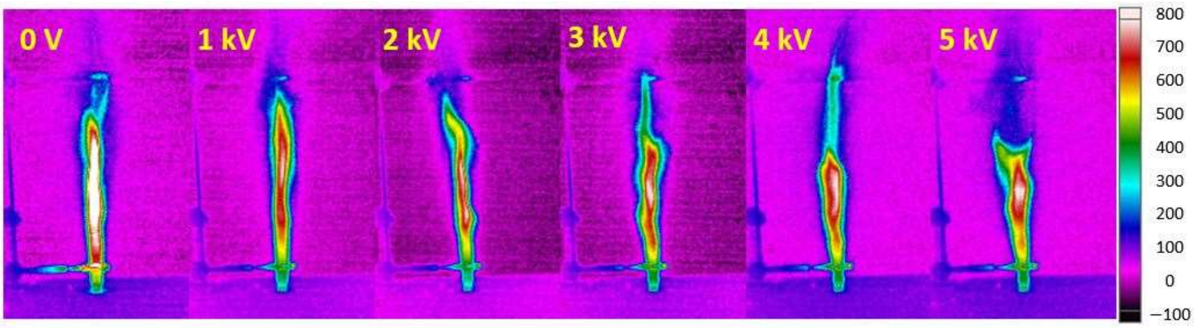

(**c**) Fuel-lean case (air 12 L/min, fuel 0.25 L/min).

Figure 6. Infrared image for negative polarity (°C): (**a**) stoichiometry case; (**b**) fuel-rich case; (**c**) fuel-lean case.

Figure 7 graphically presents the results of the flame length. As for the length of the flame presented numerically in this result, the maximum length from the burner surface to the part of the flame at 600 °C or higher was defined as the length of the flame. The length of 20 thermal images of the flame was measured, and the average was presented as a result.

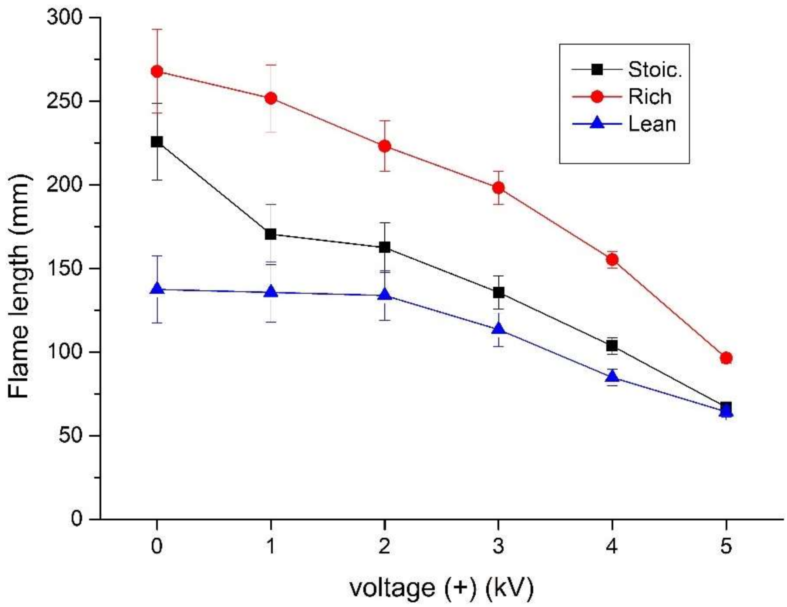

(**a**)

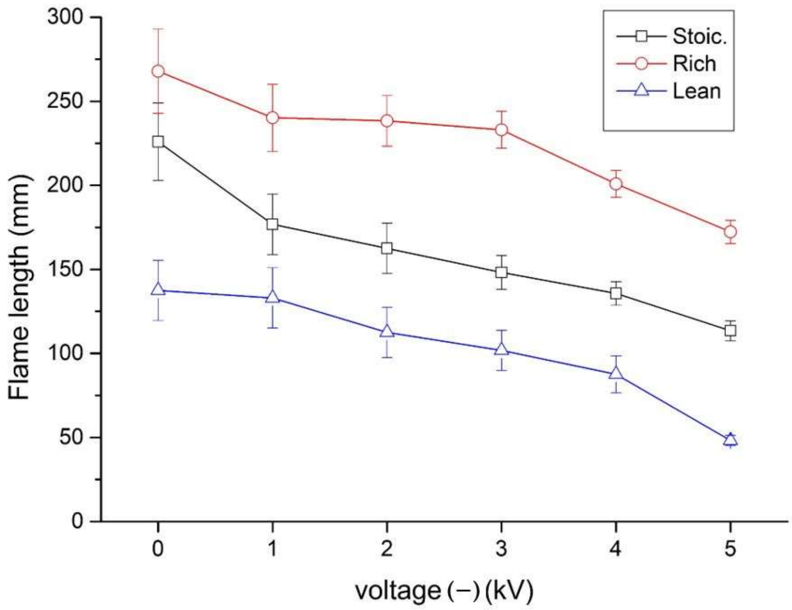

(**b**)

Figure 7. Flame length by electric field: (**a**) with positive voltage; (**b**) with negative voltage.

As shown, (a) is the result when the electrode is positively charged, and (b) is the result when the electrode is negatively charged. In the fuel-rich case, where the flow rate (Q) of the supplied fuel was double, and the air-fuel ratio (s) was small, the flame length was the longest in all cases under all voltages (Equation (1)). Additionally, the flame length of the fuel-lean case with a large air-fuel ratio was the shortest in all cases under all voltages.

In the electric field to which a positive voltage was applied, the flame length of the stoichiometry and the fuel-rich case decreased steadily as the voltage increased, and in the fuel-lean case, the flame length started to decrease sharply above 2 kV. In the fuel-lean case, it can be seen that the decrease in flame length due to the low equivalence ratio (φ = 0.5) is more dominant than the increase in the diffusion coefficient by the electric field at a low voltage of 2 kV or less.

The length of the flame continued to decrease as the voltage increased also in the electric field to which the negative voltage was applied, but the decrease was small, compared to the positive case.

Flames contain a high concentration of free electrons and charged ions. The rate of ion generation depends on the mixture composition. When the DC electric field is applied on the propane diffusion flame through the electrode, a large number of ions and electrons are moved. This ionic wind affects flame dynamics, which enhances the heat and mass transfer between the flame front and the unburned area, thereby increasing the rate of combustion. As a result, the length of the flame is reduced.

In all cases, the fuel-rich case has the longest flame length, and the fuel-lean case has the shortest. When the electrode is negatively charged, the flame length decreases by 35 to 65% at −5 kV, and by 53 to 70% at +5 kV, when positively charged.

3.2. NO_x Formation

The amount of NO_x generated from the flame was measured by inserting the suction tube of the gas analyzer into the exhaust duct for the propane diffusion flame. Here, the amount of NO_x means the sum of the amounts of NO and NO_2.

In a coaxial diffusion flame, when the same amount of fuel is burned, flame instability increases as the length of the flame increases, and soot and NO_x generation are also affected [8–11].

When the electrode is charged with positive polarity (Figure 8a) up to 2 kV at all air-fuel ratios, the amount of NO_x reduction is not noticeable. However, as the voltage continues to increase, the amount of NOx rapidly decreases up to 3.5 kV. After that, the amount of generated NO_x is almost constant even when the voltage is increased.

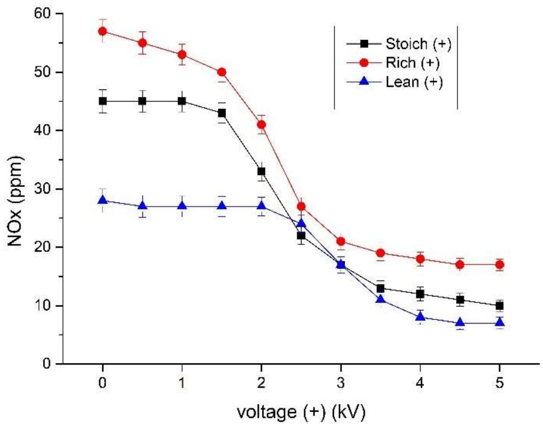

(**a**)

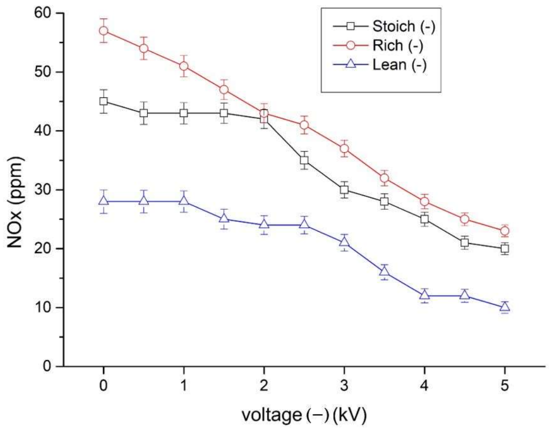

(**b**)

Figure 8. NO_x formation: (**a**) with positive voltage; (**b**) with negative voltage.

When the negative electric field is applied to the flame (Figure 8b), it is shown that the amount of NO_x production decreases steadily at all air-fuel ratios.

In both results, the main reason for the decrease in the amount of NO_x generation is that the length of the flame is decreased by the electric field, and the residential time of the flame is decreased. Thus, the chance of thermal NO_x formation is reduced.

Through this study, it is noticed that the maximum reduction in NO_x with the applied voltage and polarity is within the range of 55% to 78%. It is also noticed that the NO_x emission is gradually decreased with an increase in the applied voltage (0 to 5 kV) for both polarities (positive and negative).

3.3. EINOx Scaling

Peters and Donnerhack [10] derived theoretical equations for emission index of NOx (EINOx), grams of nitrogen oxides produced per kilogram of fuel), and the length of diffusion flame (Equation (7)), Chen [28] and Driscoll [29] derived a relational expression shown in Equation (8), after revising it in Equation (7), considering the effect of the turbulence of the flame. After that, Equations (7) and (8) were experimentally verified by the researchers in models of several diffusion flames [11,30–33].

$$EINO_x \sim \left(\frac{L_f^3}{d_F^2 U_F}\right) \tag{7}$$

$$EINO_x \sim \left(\frac{L_f^3}{d_F^2 U_F}\right)\left(\frac{U_F}{d_F}\right)^{1/2} \tag{8}$$

In Equations (7) and (8), L_f is the length of the flame, d_f is the diameter of the fuel nozzle, and U_f is the fuel outlet velocity. As seen in the equations, $EINO_x$ scales the length of the flame to the power of three; that is, the amount of NO_x generated is most affected by the length of the flame. In each case of this experimental study, U_f and d_f are fixed, and only L_f changes by the electric field. Therefore, in Equation (8), $\left(\frac{U_F}{d_F}\right)^{1/2}$ is regarded as constant.

Figure 9 is a graph drawn by substituting the $EINO_x$ result according to the flame length into Equation (7) when the electric field is used. In the graph, the slope of the average line is 0.35. This can be expressed as follows:

$$EINO_x \sim \left(\frac{L_f^3}{d_F^2 U_F}\right)^{0.35} \tag{9}$$

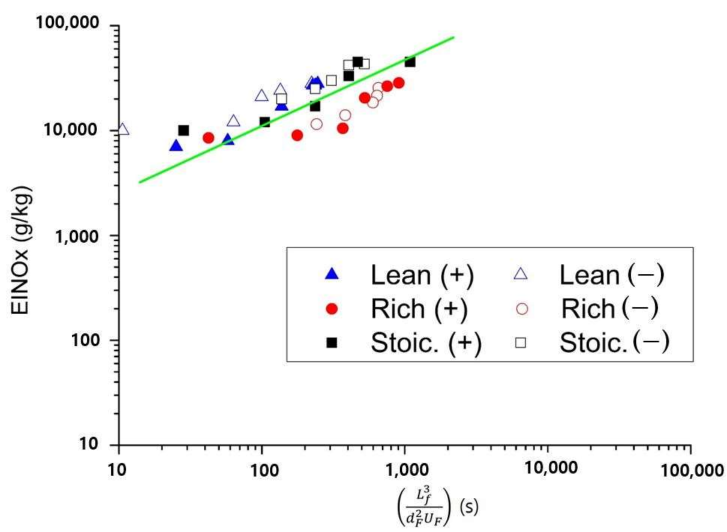

Figure 9. EINOx normalized by flame length.

Compared to Equation (7), Equation (9) shows that $EINO_x$ is smaller by 0.35 power, which indicates that a smaller amount of NO_x is generated in the flame with the electric field.

4. Conclusions

In order to observe the effect of the electric field generated in the direction parallel to the flame, the electric field was generated by applying ±5 kV DC voltage to the ring-type electrode around the flame. Using a thermal imaging camera and a gas analyzer, the length of the flame and the amount of nitrogen oxide produced were measured according to the size and direction of the electric field. As the voltage increased, the length of the flame was sharply shortened due to the increase in the diffusion coefficient of ions in the flame. As the length of the flame was shortened, the amount of NO_x produced due to the decrease in the residence time of the flame also decreased. The fuel-rich case had the longest, and the fuel-lean case had the shortest length of the flame with no voltage and electric field applied. When the electrode was negatively charged, the length of the flame decreased by 35 to 65% at −5 kV, and when positively charged, it decreased by 53 to 70% at +5 kV. NO_x generation decreased by 55~64% at −5 kV and 70~77% at +5 kV. On a logarithmic scale, the slope of the flame length to the cube and $EINO_x$ was 0.35, and this result indicates that having the same flame length, the amount of NO_x generation in the flame with the electric field is lower than without it.

Author Contributions: Conceptualization, S.-W.B. and S.-M.K.; methodology, S.-W.B. and S.-M.K.; software, S.-M.K.; validation, S.-M.K.; and K.-S.H.; formal analysis, S.-M.K. and K.-S.H.; investigation, S.-M.K. and K.-S.H.; resources, S.-W.B.; data curation, S.-M.K. and K.-S.H.; writing—original draft preparation, S.-M.K.; writing—review and editing, S.-M.K. and K.-S.H.; visualization, S.-M.K.; supervision, S.-W.B.; project administration, S.-W.B.; funding acquisition, S.-W.B.; All authors have read and agreed to the published version of the manuscript.

Funding: This work was supported by the National Research Foundation of Korea (NRF) grant funded by the Korean government (Ministry of Science, ICT) (No. 2017M2A8A4015277).

Institutional Review Board Statement: Not applicable.

Informed Consent Statement: Not applicable.

Data Availability Statement: Not applicable.

Conflicts of Interest: The authors declare no conflict of interest.

References

1. Calcote, H.F.; Keil, D.G. Ion-molecule reactions in sooting acetylene oxygen flames. *Combust. Flame* **1988**, *74*, 131–146. [CrossRef]
2. Eraslan, A.N.; Brown, R.C. Chemiionization and ion molecule reactions in fuel-rich acetylene flames. *Combust. Flame* **1988**, *74*, 19–37. [CrossRef]
3. Fialkov, A.B. Investigations on ions in flames. *Prog. Energy Combust. Sci.* **1997**, *23*, 399–528. [CrossRef]
4. Pederson, T.; Brown, R.C. Simulation of electric field effects in premixed methane flames. *Combust. Flames* **1993**, *94*, 433–448. [CrossRef]
5. Berman, C.H.; Gill, R.J.; Calcote, H.F. *NOx Reduction in Flames Stabilized by an Electric Field*; American Society of Mechanical Engineers Petroleum Division: New York, NY, USA, 1991.
6. Glassman, I. *Combustion*; Academic Press: Cambridge, MA, USA, 2014.
7. Collins, M.M.; Cooper, C.D.; Dietz, J.D.; Clausen, C.A., III; Tazi, L.M. Pilot-scale evaluation of H_2O_2 injection to control NOx emissions. *J. Environ. Eng.* **2001**, *127*, 329–336. [CrossRef]
8. Roper, F.G.; Smith, C.; Cunningham, A.C. The prediction of laminar jet diffusion flame sizes: Part II. Experimental verification. *Combust. Flame* **1977**, *29*, 227–234. [CrossRef]
9. Roper, F.G. The prediction of laminar jet diffusion flame sizes: Part I. Theoretical model. *Combust. Flame* **1977**, *29*, 219–226. [CrossRef]
10. Peters, N.; Donnerhack, S. Structure and similarity of nitric oxide production in turbulent diffusion flames. *Symp. Int. Combust.* **1981**, *18*, 33–42. [CrossRef]
11. Weiland, N.; Chen, R.H.; Strakey, P. Effects of coaxial air on nitrogen-diluted hydrogen jet diffusion flame length and NOx emission. *Proc. Combust. Inst.* **2011**, *33*, 2983–2989. [CrossRef]
12. Barmina, I. Active electric control of emissions from swirling combustion. In *Advanced Combustion and Aerothermal Technologies*; Springer: Dordrecht, The Netherlands, 2007; pp. 405–412.

13. Heinsohn, R.J.; Wilhelm, C.F., Jr.; Becker, P.M. Effect of electric fields on ducted diffusion flames. *Combust. Flame* **1970**, *14*, 341–349. [CrossRef]
14. Fang, J.; Wu, X.; Duan, H.; Li, C.; Gao, Z. Effects of electric fields on the combustion characteristics of lean burn methane-air mixtures. *Energies* **2015**, *8*, 2587–2605. [CrossRef]
15. Barmina, I.; Kolmickovs, A.; Valdmanis, R.; Zake, M. Control of combustion dynamics by an electric field. *Chem. Eng. Trans.* **2015**, *43*, 973–978.
16. Won, S.H.; Ryu, S.K.; Kim, M.K.; Cha, M.S.; Chung, S.H. Effect of electric fields on the propagation speed of tribrachial flames in coflow jets. *Combust. Flame* **2008**, *152*, 496–506. [CrossRef]
17. Marcum, S.D.; Ganguly, B.N. Electric-field-induced flame speed modification. *Combust. Flame* **2005**, *143*, 27–36. [CrossRef]
18. Borgatelli, F.; Dunn-Rankin, D. Behavior of a small diffusion flame as an electrically active component in a high-voltage circuit. *Combust. Flame* **2012**, *159*, 210–220. [CrossRef]
19. Chahine, M.; Gillon, P.; Sarh, B.; Blanchard, J.N.; Gilard, V. Stability of a laminar jet diffusion flame of methane in an oxygen enriched air co-jet. In Proceedings of the Seventh Mediterranean Combustion Symposium, Sardinia, Italy, 11–15 September 2011.
20. Viehland, L.A.; Mason, E.A. Gaseous ion mobility and diffusion in electric fields of arbitrary strength. *Ann. Phys.* **1978**, *110*, 287–328. [CrossRef]
21. Whealton, J.H.; Mason, E.A. Transport coefficients of gaseous ions in an electric field. *Ann. Phys.* **1974**, *84*, 8–38. [CrossRef]
22. Kim, S.M.; Jyoti, B.V.S.; Baek, S.W.; Kyritsis, D.C.; Ghim, Y.C. Effects of Electrostatic Voltage and Polarity on Diffusion-Controlled Propane Flame for Enhanced Efficiency. 2018. Available online: https://ascelibrary.org/doi/10.1061/%28ASCE%29EY.1943-7897.0000524. (accessed on 6 September 2021).
23. Chien, Y.C.; Dunn-Rankin, D. Electric field induced changes of a diffusion flame and heat transfer near an impinging surface. *Energies* **2018**, *11*, 1235. [CrossRef]
24. Farraj, A.R.D.; AL-Naeemy, A.M.; Al-Khateeb, A.N.; Kyritsis, D.C. Laminar non-premixed counterflow flames manipulation through the application of external direct current fields. *J. Energy Eng.* **2017**, *143*, 1–8. [CrossRef]
25. Pu, Z.; Zhou, C.; Xiong, Y.; Wu, T.; Zhao, G.; Yang, B.; Li, P. Two dimensional axisymmetric simulation analysis of vegetation combustion particles movement in flame gap under DC voltage. *Energies* **2019**, *12*, 3596. [CrossRef]
26. Chen, R.H.; Driscoll, J.F. Nitric oxide levels of jet diffusion flames: Effects of coaxial air and other mixing parameters. *Symp. Int. Combust.* **1991**, *23*, 281–288. [CrossRef]
27. Li, C.; Wu, X.; Li, Y.; Hou, J. Deformation study of lean methane-air premixed spherically expanding flames under a negative direct current electric field. *Energies* **2016**, *9*, 738. [CrossRef]
28. Driscoll, J.F.; Chen, R.H.; Yoon, Y. Nitric oxide levels of turbulent jet diffusion flames: Effects of residence time and Damkohler number. *Combust. Flame* **1992**, *88*, 37–49. [CrossRef]
29. Chen, J.Y.; Kollmann, W. PDF modeling and analysis of thermal NO formation in turbulent nonpremixed hydrogen-air jet flames. *Combust. Flame* **1992**, *88*, 397–412. [CrossRef]
30. Turns, S.R. Understanding NOx formation in non-premixed flames: Experiments and modeling. *Prog. Energy Combust. Sci.* **1995**, *21*, 361–385. [CrossRef]
31. Sanders, J.P.H.; Chen, J.Y.; Gökalp, I. Flamelet-based modeling of NO formation in turbulent hydrogen jet diffusion flames. *Combust. Flame* **1997**, *111*, 1–15. [CrossRef]
32. Kim, S.H.; Yoon, Y.; Jeung, I.S. Nitrogen oxides emissions in turbulent hydrogen jet non-premixed flames: Effects of coaxial air and flame radiation. *Proc. Combust. Inst.* **2000**, *28*, 463–471. [CrossRef]
33. Oh, J.; Heo, P.; Yoon, Y. Acoustic excitation effect on NOx reduction and flame stability in a lifted non-premixed turbulent hydrogen jet with coaxial air. *Int. J. Hydrog. Energy* **2009**, *34*, 7851–7861. [CrossRef]